Eur. J. Mineral.
2003, **15**, 893–901

Computer simulation of Al-Mg ordering in glaucophane and a comparison with infrared spectroscopy

ERIKA J. PALIN[1]*, BETH S. GUITON[1,2], MARTIN S. CRAIG[1,3], MARK D. WELCH[1,4], MARTIN T. DOVE[1] and SIMON A.T. REDFERN[1]

[1]Department of Earth Sciences, University of Cambridge, Downing Street, Cambridge, CB2 3EQ, UK
*Corresponding author: e-mail: ejp24@cam.ac.uk
[2]Present address: Harvard University, Department of Chemistry and Chemical Biology, 12 Oxford Street, Cambridge, MA 02138, USA
[3]Present address: Rutherford Appleton Laboratory, Chilton, Didcot, Oxfordshire OX11 0QX, UK
[4]Department of Mineralogy, Natural History Museum, Cromwell Road, London, SW7 5BD, UK

Abstract: The ordering of Mg and Al over the octahedral sites in glaucophane, $^{[A]}\square^{[8]}Na_2{}^{[6]}(Mg_3Al_2)^{[4]}Si_8O_{22}(OH)_2$, has been studied by Monte Carlo simulation using a model Hamiltonian parameterised using both empirical interatomic interactions and *ab initio* calculations. It is found that Al is fully ordered at the M(2) site, with disorder beginning to appear for temperatures above ~1000 K. Infrared spectra of three synthetic high-PT glaucophane-nyböite amphiboles were also collected and the OH-stretching frequencies used to infer the state of Al-Mg ordering. The spectra of all three amphiboles comprise only two peaks at ~3662 cm^{-1} and ~3720 cm^{-1}, corresponding to MgMgMg–OH–$^{[A]}\square$ and MgMgMg–OH–$^{[A]}$Na, respectively. These infrared spectra show unequivocally that M(1) and M(3) sites are fully occupied by Mg, and, therefore, $^{[6]}$Al is fully ordered at M(2), in agreement with the behaviour predicted by the computational studies and bond-valence considerations.

Such a highly $^{[6]}$Al-ordered state for alkali amphiboles contrasts starkly with calcic amphiboles synthesized under similar pressure-temperature conditions, which have a high degree of $^{[6]}$Al disorder over M(2) and M(3) sites. This difference between alkali and calcic amphiboles shows the major influence that the M(4) cation (monovalent *versus* divalent) has, via its bonding relations to O(4), in controlling the ordering of trivalent cations over the octahedral sites in amphiboles.

Key-words: glaucophane, cation ordering, Monte Carlo simulations, *ab initio* calculations, infrared spectroscopy.

Introduction

As part of a wider investigation into cation ordering in minerals, we present in this paper a study of cation ordering in the amphibole glaucophane, $^{[A]}\square^{[8]}Na_2{}^{[6]}(Mg_3Al_2)^{[4]}Si_8O_{22}(OH)_2$. In previous work, we have studied Al/Si ordering in muscovite (Palin *et al.,* 2001), in which ordering occurs essentially in two dimensions within each tetrahedral phyllosilicate sheet; Al/Si and Al/Mg ordering in phengite (Palin *et al.,* 2003), in which the networks of tetrahedral and octahedral sheets are able to exchange Al but the Si and Mg are restricted to [4] and [6] sites respectively; and Al/Fe/Mg ordering in octahedral illite/smectite sheets (Sainz-D´az *et al.,* 2003a, b), which was an important step towards realistic mineral systems in view of the presence of three ordering species.

Our motivation in this study is to examine a different issue – namely, the behaviour of a system in which the ordering cations are able to move between networks of different sites. This is termed non-convergent ordering, since the sites in one network are not equivalent to those in another, and hence complete disorder over all sites at high temperature is never attained. Non-convergent ordering has been studied in other mineral systems, including spinels and orthopyroxene (Carpenter *et al.,* 1994a) and potassium feldspar (Carpenter *et al.,* 1994b).

The amphibole structure (Fig. 1) also lends itself well to the study of non-convergent ordering. It comprises ribbons of edge-sharing octahedrally coordinated cations sandwiched between two double-chains of tetrahedral sites (Al, Si), forming the so-called "I-beam" unit. Adjacent I-beams are connected via a distorted six- or eight-coordinated cation site, M(4), to form a chequer-board array in which I-beams alternate with large continuous channels. The channel site (hereafter "*A*" site) can be vacant, full or partially occupied by large cations Na^+, K^+, Ca^{2+} and Pb^{2+} in [10]–[12] coordination. There are seven distinct types of cation site: three regular octahedral sites M(1,2,3), the distorted octahedral or cube-octahedral M(4) site, the *A* site and two types of tetrahedral sites, T(1,2). There are two

0935-1221/03/0015-0893 $ 4.05
DOI: 10.1127/0935-1221/2003/0015-0893

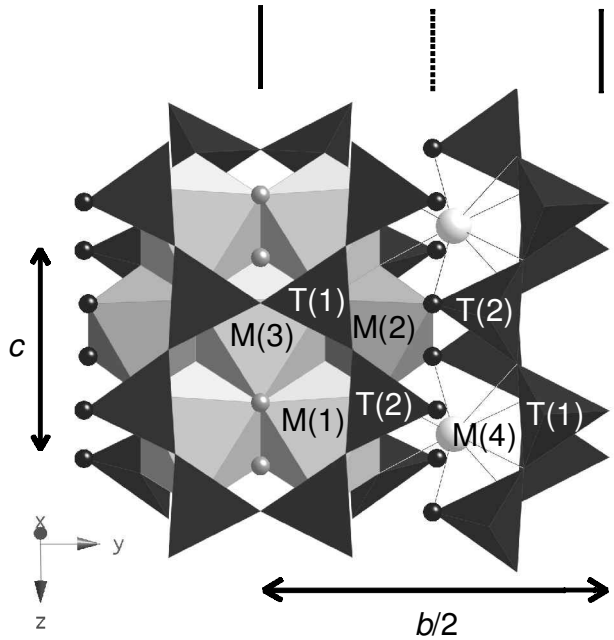

Fig. 1. Glaucophane structure viewed along the *x*-axis, indicating location of T and M sites. The hydroxyl groups, bonded to two M(1) and one M(3) sites, are indicated by small grey spheres. Solid lines at the top of the figure indicate mirror planes and the broken line indicates an *a*-glide plane. The O(4) atoms, which are important in constraining the occupancy of the M(2) sites by bond valence considerations, are indicated by small black spheres.

M(1,2,4) sites, one M(3) site, four T(1,2) sites, one *A* site and two OH^- per formula unit. The M(1) and M(3) cations are *cis*- and *trans*-bonded to two OH^- groups, respectively; M(2) is not bonded to OH^-. The M(1,2,3) octahedra can be occupied by divalent and trivalent cations, and also Li^+ (at M(3)). In most natural compositions, the main divalent cations are Mg, Fe^{2+}, Mn^{2+}, and the significant trivalent cations are Al, Fe^{3+}, Mn^{3+}. The M(4) site, being larger and more flexible than the M(1,2,3) sites, accommodates Na^+, Ca^{2+} and Mn^{2+} as well as smaller Mg^{2+} and Fe^{2+} cations. The main amphibole groups are defined by their M(4) chemistries (calcic, sodic-calcic, alkali, Mg-Fe-Mn amphiboles), reflecting the primary significance of this cation site in the amphibole structure.

The variety of cation sites within the amphibole structure, along with its inherent structural flexibility, allows an enormous range of chemical substitutions to occur, making these minerals among the chemically most diverse and structurally complex of minerals. Furthermore, the chemical voracity of amphibole is responsible for its occurrence in a wide range of rock compositions and its stability under a wide range of pressure and temperature. As such, amphiboles have the potential to provide detailed petrological histories of their parent rocks (geothermobarometry, geospeedometry), provided that pressure-temperature-time dependencies of amphibole compositions, cation ordering and microstructures can be quantified and interpreted. As demonstrated by Hawthorne (1997), bond-valence theory provides a particularly comprehensive crystal-chemical explanation of the long- and short-range ordering of cations within amphibole. Bond-valence effects are essentially enthalpic in character, reflecting bond energetics. Here, we present the first step in developing a quantitative model of the energetics underlying the bond-valence description of cation ordering in amphiboles.

In this work we consider end-member glaucophane, $^{[A]}\square^{[8]}Na_2{}^{[6]}(Mg_3Al_2)^{[4]}Si_8O_{22}(OH)_2$, in which the *A* site is vacant, M(4) is completely filled with Na, the tetrahedral sites contain Si only, and the only possible sites upon which cations can order are the M(1,2,3) sites which contain a total of two Al and three Mg. This amphibole composition was chosen for its chemical simplicity, as we are here focusing upon understanding the long-range ordering of Mg and Al just over the octahedral M(1,2,3) sites. Other compositions, such as magnesio-hornblende, $^{[A]}\square^{[8]}Ca_2{}^{[6]}(Mg_4Al)^{[4]}(Si_7Al)O_{22}(OH)_2$, with tetrahedral and octahedral Al are more challenging in that account must also be taken of coupling between octahedral and tetrahedral Al ordering (Mg/Al and Al/Si).

A bond-valence analysis of cation ordering at M(1,2,3) sites (*e.g.* Hawthorne, 1997) reveals that trivalent cations are likely to order strongly at the M(2) site in order to reduce the "underbonding" of the three-coordinated O(4) atom bonded to M(2), M(4) and T(2). For end-member glaucophane, the Pauling bond strength of this anion when M(2) = Mg is only 1.46 valence units, *vu*, coming from $^{[8]}$Na at M(4) (0.13 *vu*), $^{[6]}$Mg (0.33 *vu*) and $^{[4]}$Si at T(2) (1.00 *vu*). When M(2) = Al, the bond strength increases to a more respectable 1.67 *vu*. Structurally, this state of affairs is reflected in short $^{[6]}$Al–O(4) and Si–O(4) bonds.

Interestingly, for high-temperature (> 1000 K) natural and synthetic aluminous calcic amphiboles (*e.g.* pargasite, magnesio-hornblende), there is strong spectroscopic and diffraction evidence for considerable disorder of Al over M(2) and M(3) sites (Welch *et al.,* 1994; Oberti *et al.,* 1995; Jenkins *et al.,* 1997; Welch & Knight, 1999; Hawthorne *et al.,* 2000), which for the compositions studied implies that significant amounts of divalent cations occur at M(2), thus violating the "dictates" of bond-valence analysis. This means that at high temperatures there is an increasingly favourable contribution to the Gibbs free energy from configurational entropy arising from cation disorder. It is possible to model this burgeoning entropic contribution to cation site-exchange energetics, as we have demonstrated previously (see *e.g.* our muscovite work, Palin *et al.,* 2001).

Methods

Basic approach to computer simulations

Our method for simulating cation ordering processes comprises two stages. The first stage involves calculating values for ordering interactions by using empirical interatomic potentials and lattice energy relaxation methods. The second stage uses these values to simulate ordering as a function of temperature via Monte Carlo simulations. Our approach uses a model Hamiltonian for the ordering interactions (stage one); we refer to this as the *J* formalism. Both the *J* formalism and our Monte Carlo methods (stage two) have

Table 1. Parameters used in interatomic potentials for GULP.

Potential type	Atoms	Parameter values				
		A	ρ	*C*	r_{max}	
Buckingham	Si core – O shell[1]	1283.9074	0.3205	10.662	8	
Buckingham	Al core – O shell[1]	1460	0.29912	0	8	
Buckingham	Mg core – O shell[1]	1428.5	0.2945	0	12	
Buckingham	Na core – O shell[2]	1226.84	0.3065	0	10	
Buckingham	O shell – O shell[1]	22764	0.149	27.88	12	
Buckingham	H core – O shell[1]	311.97	0.25	0	8	
		K				
Spring (core-shell)	O core – O shell[1]	74.92				
		k	θ_0	r_{max} (1–2)	r_{max} (2–3)	r_{max} (1–3)
Three-body	O shell – Si core – O shell[1]	2.0972	109.47	1.8	1.8	3.2
Three-body	O shell – Al2 core – O shell[1]	2.0972	90	2.2	2.2	3.2
Three-body	O shell – Mg core – O shell[3]	2.0972	90	2.2	2.2	3.2

[1]From Winkler *et al.* (1991)
[2]From Catlow *et al.* (1984)
[3]From Sainz-D´az *et al.* (2001)

been discussed in detail elsewhere (Bosenick *et al.,* 2001, Warren *et al.,* 2001). Here we simply quote the equation for the energy of the system:

$$E = E_0 + \sum_n N^n_{Al-Al} J^n - \mu N x \quad (1)$$

The first term in this expression is a constant which is not relevant to studies of ordering. The second term depends on the number of Al–Al bonds, and the exchange interaction parameter J, which is defined as $J = E_{Al-Al} + E_{Mg-Mg} - 2\,E_{Al-Mg}$ in the case of Al–Mg order. This term has to be summed over all n, *i.e.* over all different types of neighbours. The final term is a chemical potential term, included because of the possibility of Al preferring one type of site to another. μ is the chemical potential, N the total number of sites, and x the fraction of Al atoms. We note that for n different types of site, there are n–1 independent chemical potential terms. Hence, for the three octahedral sites M(1,2,3) in glaucophane, we only require two chemical potentials.

The model for glaucophane considers the interactions between octahedral sites, J_{O-O}. However, it is also necessary to include chemical potential terms associated with the M sites, since there are three non-equivalent sites, and Al could order onto any of these. Additionally, we can arbitrarily set one of the chemical potential terms to zero, because of the dependence of these terms on each other.

For the Monte Carlo simulations, we can express the energy in a slightly different form:

$$H = \sum_{<i,j>} J_{ij} S_i S_j + \sum_j \mu_j S_j \quad (2)$$

The brackets <...> indicate that no bond is counted twice. The first term accounts for the energy associated with the bonds, and the second term is a chemical potential term. J_{ij} once again denotes an exchange interaction parameter and S is a site variable defined to be 1 if the site is occupied by Al and zero otherwise. This equation is hence equivalent to Equation 1, ignoring the E_0 term, which is not relevant to the ordering process.

In addition to our usual method, we have employed the use of *ab initio* calculations to assist in the calculation of chemical potential terms. This is discussed below.

Model interatomic potentials and testing

Table 1 shows the values of the parameters in the empirical interatomic potentials used to model glaucophane. The formulae for the different potentials have been quoted elsewhere (see, for example, Palin *et al.,* 2001). Energy minimisation calculations were performed using GULP (Gale, 1997).

The model was compared to cell parameter/atomic coordinates data for glaucophane from single-crystal X-ray diffraction (Papike & Clark, 1968) and cell parameter data from powder X-ray diffraction (Holland, 1988). The hydrogen atoms were not located by experiment, so they were added to the structure at suitable coordinates (the exact positions were not important, since relaxation of the structure should move the hydrogen atoms to their correct locations).

The model was tested for both disordered and ordered cases. The disordered case employed the virtual crystal approximation (VCA) whereby we represent disorder by assigning to each site available for ordering a virtual occupancy corresponding to the statistically disordered (high-temperature) case. Here, this means that all octahedral sites contain 0.4 Al and 0.6 Mg. The ordered case was based on the Papike & Clark sample, in which the M(2) sites were determined experimentally to contain Al and the M(1,3) sites Mg. Table 2 shows the comparison between the two experiments and the ordered and disordered models, together with the largest model/experiment discrepancies. There is good agreement between all experimental and calculated parameters, particularly for the ordered model.

Determination of exchange interaction parameters

A total of fourteen distances were assigned to different J_{O-O} parameters, in ascending order of distances. These are given in Table 3, together with information about the type of interaction (*i.e.* whether it is within one ribbon or between two ribbons). Fig. 2 and 3 show the locations of examples of these distances within the crystal structure.

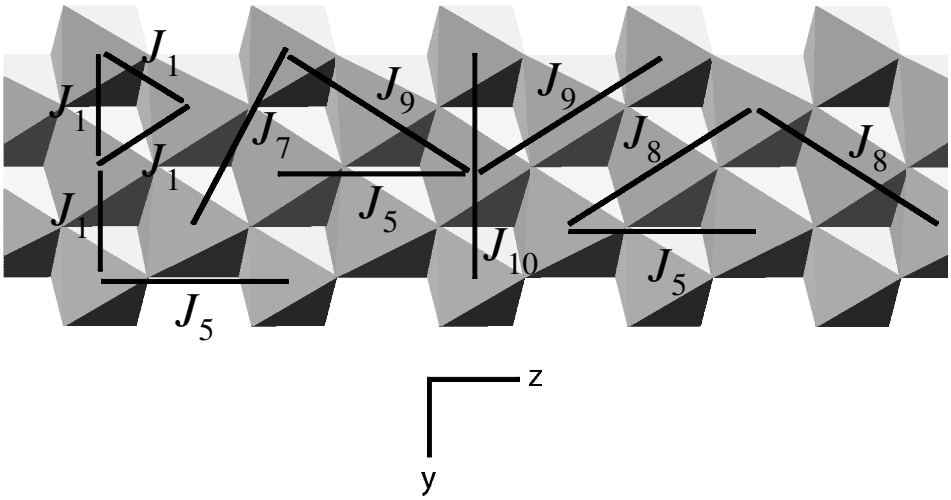

Fig. 2. One ribbon of octahedral sites showing the distances corresponding to the intra-ribbon J parameters. Linkages marked as "J_1" indicate J_1–J_4 distances (which, though initially assigned separately, were subsequently grouped).

Table 2. Comparison between experimental data and model data for glaucophane.

	Experimental data		Model data		
Parameter	Papike & Clark (1968)	Holland (1988)	Disordered (VCA)	Ordered (^{M1}Mg ^{M2}Al^{M3}Mg)	Largest % diff. between experiment and model
a (Å)	9.541	9.549	9.689	9.500	1.5
b (Å)	17.740	17.739	17.668	17.592	–0.8
c (Å)	5.295	5.294	5.267	5.309	–0.5
β(°)	103.67	103.72	105.33	104.65	1.6
<Mg–O> (Å)	2.091		2.021	2.078	–3.5
<Al–O> (Å)	1.944		2.021	1.906	3.8

Table 3. Assigned J parameters.

Parameter	Distance (Å)	Type	Value (eV)
J_1	3.077	Within ribbon	0.603
J_2	3.098	Within ribbon	"
J_3	3.107	Within ribbon	"
J_4	3.148	Within ribbon	"
J_5	5.313	Within ribbon	0.205
J_6	5.369	Inter-ribbon	–0.025
J_7	5.400	Within ribbon	0.234
J_8	6.155	Within ribbon	0.209
J_9	6.176	Within ribbon	0.210
J_{10}	6.296	Within ribbon	0.204
J_{11}	6.325	Inter-ribbon	0.015
J_{12}	6.652	Inter-ribbon	0.013
J_{13}	7.267	Inter-ribbon	–0.013
J_{14}	7.381	Inter-ribbon	0.009

To calculate the J values, we formed a 2×1×2 supercell (40 octahedral sites, 328 atoms in total) with periodic boundary conditions, and calculated the energy of many different configurations with the ordering cations placed randomly on the octahedral sites. Some ordered and partially ordered configurations were included.

We generated 90 configurations using a spreadsheet method (Bosenick *et al.*, 2001); to give us an adequate data set (typically we calculate between 50 and 100 configurations). 16 Al atoms and 24 Mg atoms were placed at random on the 40 octahedral sites, and the configurations were optimised using GULP. The lattice parameters used for these configurations were those from the previous relaxation run which employed the virtual crystal approximation. The 90 resulting lattice energies formed a set of E values in Equation 1.

The number of Al–Al interactions was determined using the spreadsheet method, for each exchange pair for each configuration. This provides 90 sets of non-zero values for $N_{\text{Al–Al}}$ for each J, which were then used in conjunction with the E values to determine values for J and the chemical potentials by linear regression, according to Equation 1.

The fit was achieved in three stages: the first stage was fitting the values of the intra-ribbon Js and chemical potential values with the E values to produce a set of intermediate E values. Next, the differences between these intermediate E values and the original E values were fitted to the inter-ribbon Js, to produce another set of intermediate E values. Finally, the differences between these last intermediate E values and the original E values were used to repeat the regression on the intra-ribbon Js. This procedure is designed to avoid correlation effects between the J values. The calculated J values are given in Table 3, and the agreement between the energies and those from GULP is shown in Fig. 4a. The correlation coefficient R^2 is 0.86.

In practice, it was found that the values of the chemical potentials μ_1 and μ_3 were fitting to very similar values, and so in the fitting procedure described above, we also applied the constraint that $\mu_1 = \mu_3$. In recalling that the three chemical potentials are not independent, we then set $\mu_1 = \mu_3 = 0$ and only fitted the value of μ_2.

The μ_2 value of 0.362 eV determined during the fitting was felt to be implausible on the following grounds. From the bond valence considerations outlined above, it is unlikely that M2 will contain Mg, which is what is implied by a positive value of μ_2. We believe that the positive value of μ_2 is an artefact of the empirical model, and so we decided to perform *ab initio* calculations on some of the structures in order to calculate a more accurate value for μ_2.

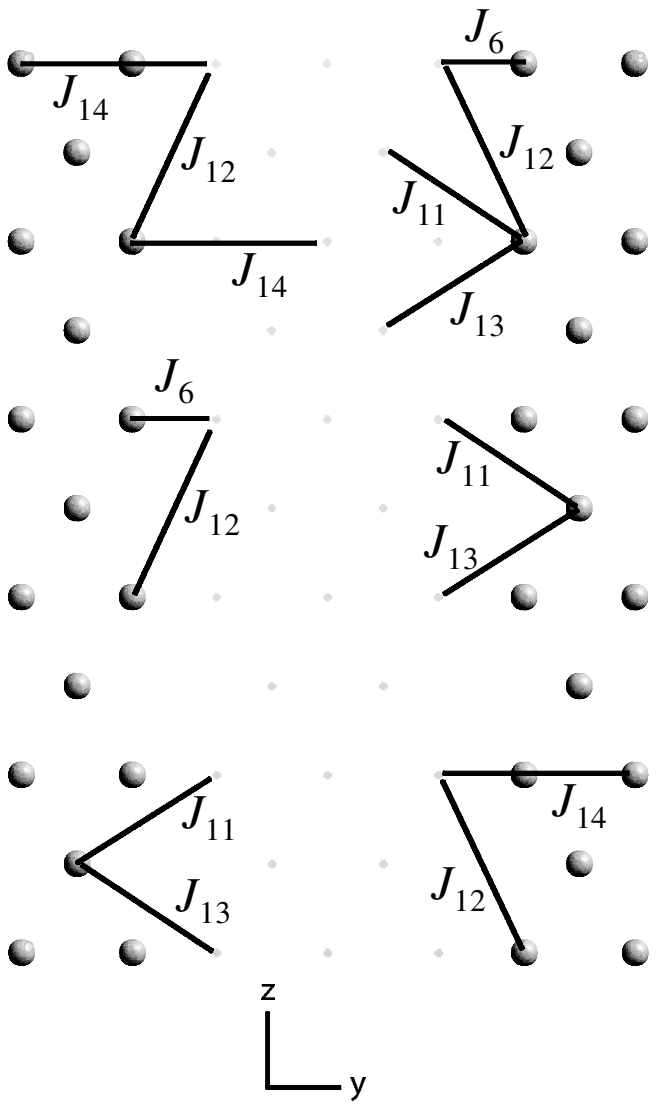

Fig. 3. Distances corresponding to the inter-ribbon J parameters. Spheres and crosses denote sites in different ribbons (*i.e.* at different heights in the unit cell).

Since the J values are driven by strain effects, which are related to the sizes of the ions concerned, we believe that the J values calculated by GULP are rather more reliable. However, GULP is not as reliable in terms of absolute energies, in that the effects of bonding can sometimes be incorrectly represented, and this is why the chemical potential value from GULP is inaccurate. It is sometimes possible for chemical potentials also to be determined by strain effects, and if this were the case here, it is likely that the GULP values would have been more plausible.

SIESTA calculations

The most common method for performing *ab initio* methods in modern solid state sciences is using density functional theory (DFT). Usually the translational symmetry is exploited by using plane waves as the basis functions for the electronic wave functions. However, plane wave computations do not scale well with the system size, and would be particularly difficult for calculations of the energies of several configurations of the amphibole structure containing 328 atoms. We therefore chose to work with a linear-scaling DFT code, in this case the SIESTA code described by Soler *et al.,* (2002). This approach uses much of the technology of standard plane wave codes, including the use of pseudopotentials to describe the effects of inner core electrons and the sue of the local density and generalised gradient approximations to model exchange and correlation interactions. The main difference is the use of numerical atomic basis sets to describe the electron wavefunctions, and it is in this respect that the method can be formulated to give linear scaling with system size. Recently this approach has been tested on calculations of mineral structures (Sainz-D´az *et al.,* 2002; Craig *et al.,* 2003).

We selected a small number of independent configurations, each with a high degree of order in order to allow us to use significantly different configurations. One had all Mg in M(1), one had all Mg in M(2), others had Mg distributed across M(1) and M(2), and one had Mg in both M(2) and M(3). The exchange energies, based on the fitted exchange constants and numbers of neighbours, were computed for each configuration and subtracted from the energies of the relaxed structures calculated using SIESTA. We have made the assumption that the difference between the exchange energy and the energy of the configuration is due to differences in the value of E_0, and the energy due to the chemical potential. We set $\mu_3 = 0$ as an arbitrary origin, and adjusted the values of E_0, μ_1 and μ_2 to give the least discrepancy between the SIESTA energy and the sum of E_0, the exchange energy and the chemical potential energy. This procedure led to a level of agreement represented in Fig. 4b, with an R^2-factor of 0.9. This level of agreement supports our assumption (above) that the values of J for the empirical model are reliable. The fitted values of μ_1 and μ_2 were 0.295 and –0.176 eV, respectively. The value for μ_2 contrasts with the positive value obtained from the GULP energies; it now allows ordering of Al onto M(2) where this was not possible before. Additionally, the values of μ_1 and μ_2 are not equal by this method. Finally, it should be noted that the energy contribution from the J values is still of the same order of magnitude as that from the chemical potentials, so we cannot simply predict the behaviour of the system from the J values or chemical potentials alone.

IR spectroscopy experiments

In hydroxyamphiboles, the M(1) and M(3) cations are *cis* and *trans*-bonded, respectively, to two O(3) atoms. The hydroxyl, OH^-, can be replaced by a fluoride ion, F^-. For amphiboles, well-established correlations exist between OH stretching frequency, ν_{OH}, and the chemistry of the two M(1) and one M(3) cations bonded to hydroxyl (*e.g.* Burns & Strens, 1966; Burns & Law, 1970; Hawthorne, 1983). For example, for each Fe^{2+} substituting for Mg at M(1,3) sites there is a decrease in ν_{OH} of 15 cm^{-1}. Similarly, for each Al substituting for Mg there is a reduction of 20 (*A*-site empty) to 30 cm^{-1} ($^{[A]}$Na) (Welch *et al.,* 1994; Jenkins *et al.,* 1997).

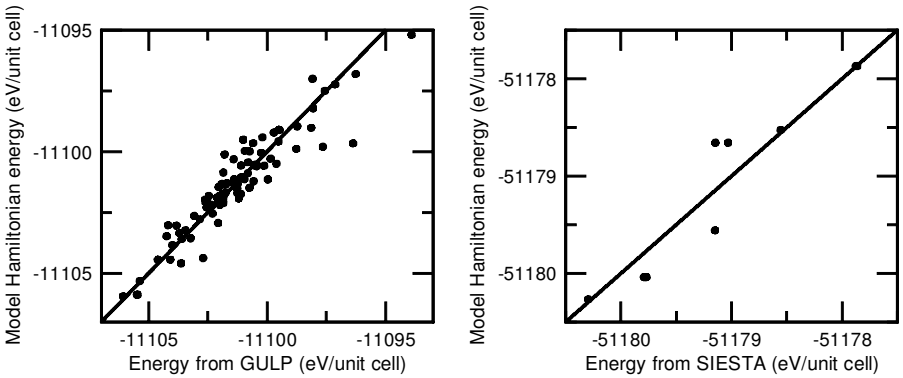

Fig. 4. (a) Plot of agreement between energies calculated using model Hamiltonian and lattice energies from GULP. (b) Plot of agreement between energies from SIESTA and energies calculated using model Hamiltonian. The straight lines on both plots indicate perfect agreement.

Table 4. Site occupancies of amphibole samples* used for IR experiments.

Sample	A	M(4)	M(1,2,3)	T(1,2)
OH/Q6	0.49Na, 0.51□	1.91Na,0.09Mg	3.17Mg, 1.83Al	7.61Si, 0.39Al
OH/Q7	0.43Na, 0.57□	1.82Na,0.18Mg	3.24Mg, 1.76Al	7.66Si, 0.34Al
GN6	0.84Na, 0.16□	1.95Na,0.05Mg	3.21Mg, 1.79Al	7.29Si, 0.71Al

* From Pawley (1992), normalised to $O_{22}(OH)_2$

The value of ν_{OH} is also affected by the contents of the *A* site: occupation of this site by Na or K increases ν_{OH} relative to an empty *A* site by about 60 cm^{-1} in amphiboles (Robert *et al.,* 1989; Della Ventura & Robert, 1990). Furthermore, for two-element compositions at octahedral sites, the occupancy of M(2) can be deduced from the occupancies of M(1,3) determined by infrared spectroscopy. Thus, vibrational spectroscopy provides essential information about the M(1,3) cation groupings around O(3)–H and, indirectly for simple compositions, the occupancy of M(2). Hawthorne *et al.* (2000) have also shown that infrared spectra of aluminous tremolites (magnesio-hornblendes) contain information about the ordering of more distant octahedral cations about O(3)–H. For amphiboles with two or three cations mixing on M(1,2,3), infrared spectra in the OH-stretching region also indirectly allow the composition of M(2) to be estimated. To take a simple example: if only peak(s) due to [MgMgMg]–OH–[A] and/or [MgMgMg]–OH–[□] is/are observed for an amphibole having a total M(1,2,3) chemistry of Mg_3Al_2, then it is obvious that $^{[6]}$Al is completely ordered at M(2). The M(4) cation appears to have a very small effect upon ν_{OH} (< 5 cm^{-1}, Hawthorne *et al.,* 1996).

We collected the infrared spectra of three amphibole samples of near-binary glaucophane-nyböite compositions synthesised by Pawley (1992). Nyböite, $^{[A]}Na^{[8]}Na_2{}^{[6]}(Mg_3Al_2)^{[4]}[Si_7Al]O_{22}(OH)_2$, is related to glaucophane by the substitution $^{[A]}Na^{[4]}Al^{[A]}\square_{-1}{}^{[4]}Si_{-1}$ in which Na fills a previously vacant *A* site and one Si is replaced by Al. The samples are as follows: OH/Q6 (x_{Gl} = 0.51, x_{Ny} = 0.31), OH/Q7 (x_{Gl} = 0.58, x_{Ny} = 0.17) and GN6 (x_{Gl} = 0.15, x_{Ny} = 0.65). The site occupancies of these are listed in Table 4. Each sample (~6 mg) was mixed with 200 mg of KBr and formed into a pellet. The pellets were dried at 120 °C for 4 days to remove adsorbed water. All measurements were taken at room temperature on a Bruker IFS 66v spectrometer. Measurements of infrared absorption were made between 250 and 4500 cm^{-1}.

Results

Monte Carlo simulations

The simulation cell used was an 8×4×8 supercell, *i.e.* a 4×4×4 supercell of the unit cell used in the GULP configurations, containing a total of 2560 octahedral sites. All of the *J* values in Table 3 were used, together with chemical potentials μ_1 and μ_2 obtained from SIESTA. Both the values for μ_1 and μ_2 determined from SIESTA and the bond valence considerations suggest that Al will order onto M(2) sites (because μ_2 is negative), and Mg will order onto M(1) and M(3) sites. The configuration with the lowest energy according to SIESTA was that with all Al on M(2), and thus all Mg on M(1,3). We therefore set up three order parameters for Mg on M(1), Al on M(2) and Mg on M(3); such that all three order parameters should tend to unity at low *T* if the SIESTA prediction is correct.

We performed a cooling run, whereby the system is started in a completely random configuration. Some snapshots of the system showing perfect order, partial order and disorder are shown in Fig. 5. As predicted, the Al orders onto the M(2) sites. The order parameter data are shown in Fig. 6a; the form of the order parameter curves is characteristic of non-convergent ordering. Each of the different M sites exhibits slightly different behaviour; at low temperature it can be seen that the first sites to exchange cation types are M(1) and M(2), since the order parameters for these sites start to decrease at roughly the same temperature, whilst the M(3) order parameter is still close to unity.

From the energy data, it is possible to calculate the entropy and the free energy using the thermodynamic integration method. This technique is discussed elsewhere (Warren *et al.,* 2001); here we simply show the entropy obtained by thermodynamic integration (Fig. 6b). The entropy shows the expected increase with increasing temperature up to the

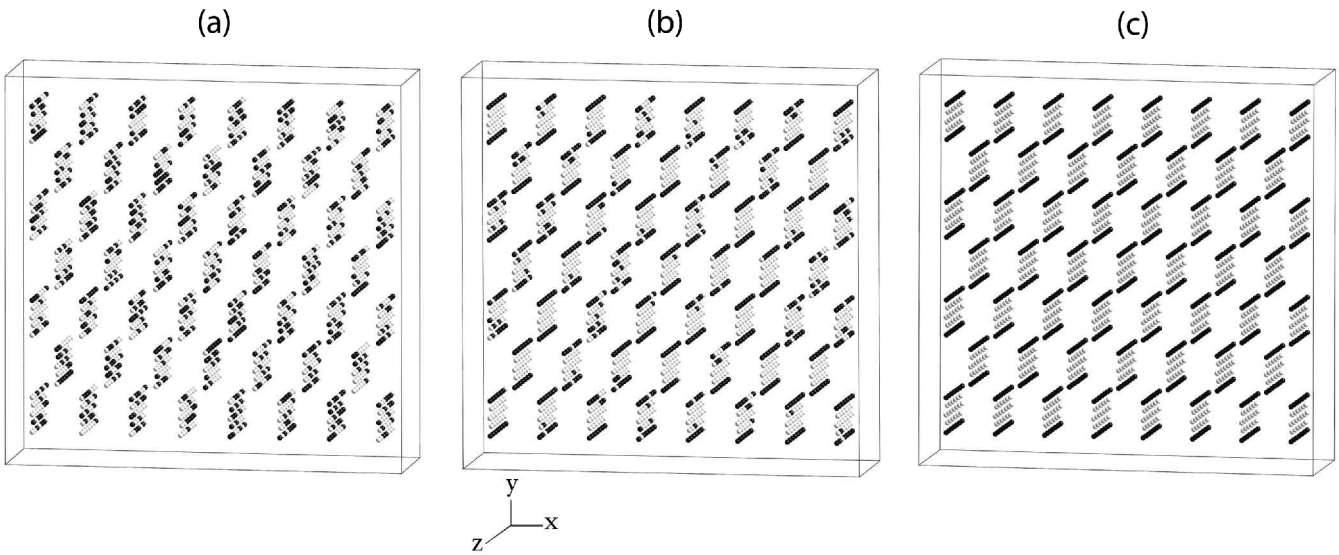

Fig. 5. Snapshots of glaucophane showing (a) complete disorder, (b) partial order and (c) perfect order. Mg are shown as light grey spheres, and Al as black spheres.

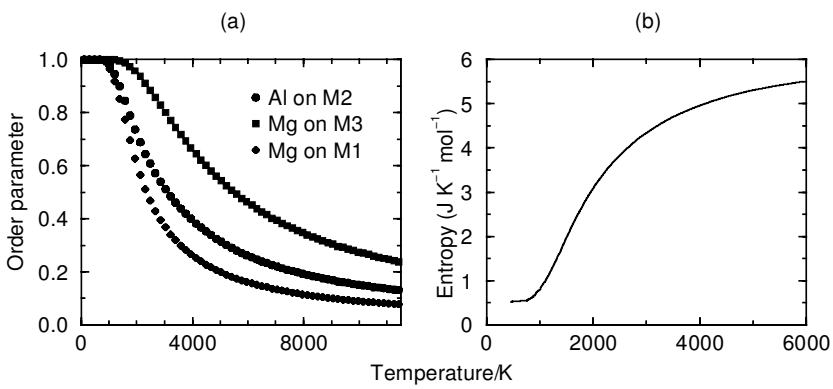

Fig. 6. (a) Order parameter data as a function of temperature. (b) Entropy as calculated by thermodynamic integration.

random value of 5.6 kJ.mol^{-1} at very high temperatures (much higher than would be attained in any experiment). In fact, at experimentally viable temperatures (< 2000 K), the system is fairly well ordered.

IR spectra

The IR spectra obtained are shown in Fig. 7 for the OH-stretching region 3550–3800 cm^{-1}. Samples OH/Q6 and OH/Q7 are very similar in composition and have similar spectra. Sample GN6 contains comparatively little glaucophane, and therefore demonstrates different behaviour.

Previous infrared spectroscopic studies have been performed on K- and Na-richterites (Robert *et al.,* 1989), (Ni, Mg, Co)-richterites (Della Ventura *et al.,* 1997), and K-richterite-tremolites (Hawthorne *et al.,* 1997). These amphiboles have only Mg on the M(1,2,3) sites, and hence any variation in peak frequencies will be dependent on the occupancy of the *A*-site. The relevant results of these studies are summarised in Table 5. From this table it can be seen that peaks around 3670–3675 cm^{-1} have previously been as-

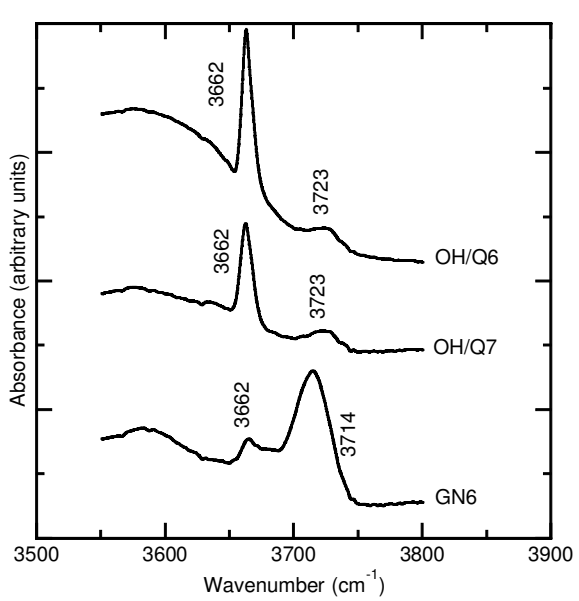

Fig. 7. IR spectra of glaucophane-bearing amphibole samples in the OH stretching region.

Table 5. Data from previous IR spectroscopy studies on Mg-bearing amphiboles.

Amphibole	Formula	ν_{OH} (cm^{-1})	Peak assignment
K-richterite[1,2]	$^{[A]}K^{[8]}(NaCa)^{[6]}Mg_5{}^{[4]}Si_8O_{22}(OH)_2$	3735, 3730*	^{A}K…MgMgMg–OH
		3670	^{A}□…MgMgMg–OH†
Na-richterite[1]	$^{[A]}Na^{[8]}(NaCa)^{[6]}Mg_5{}^{[4]}Si_8O_{22}(OH)_2$	3730	^{A}Na…MgMgMg–OH
		3670	^{A}□…MgMgMg–OH†
Tremolite[3]	$^{[A]}□^{[8]}Ca_2{}^{[6]}Mg_5{}^{[4]}Si_8O_{22}(OH)_2$	3674	^{A}□…MgMgMg–OH
Al-tremolite[4]	$^{[A]}□^{[8]}Ca_2{}^{[6]}(Mg_4Al)^{[4]}(Si_7Al)O_{22}(OH)_2$	3672	^{A}□…MgMgMg–OH
		3652	^{A}□…MgMgAl–OH
Pargasite[5]	$^{[A]}Na^{[8]}Ca_2{}^{[6]}(Mg_4Al)^{[4]}(Si_6Al_2)O_{22}(OH)_2$	3711	^{A}Na…MgMgMg–OH
		3680	^{A}Na…MgMgAl–OH

* Two peaks assigned to K in sub-sites with different point symmetries.
† This peak is due to a small deviation from the nominal end-member formula.
[1] Robert *et al.* (1989), [2] Hawthorne *et al.* (1997), [3] Hawthorne *et al.* (1996), [4] Jenkins *et al.* (1997), [5] Welch *et al.* (1994).

signed to MgMgMg–OH–$^{[A]}$□ and peaks around 3730–3735 cm^{-1} to [MgMgMg]–OH–$^{[A]}$Na.

Based on these observations, we can assign the peaks in the spectra in Fig. 7. We therefore assign the peaks at ~3662 cm^{-1} to MgMgMg–OH adjacent to a vacant A-site, and those at ~3720 cm^{-1} to MgMgMg–OH with $^{[A]}$Na. In GN6 the MgMgMg–OH–$^{[A]}$Na peak is more intense than the MgMgMg–OH–$^{[A]}$□ peak, whereas the reverse is true of OH/Q6 and OH/Q7. Undoubtedly, this difference is due to GN6 containing more $^{[A]}$Na than OH/Q6 and OH/Q7. Infrared spectra of synthetic pargasite, $^{[A]}Na^{[8]}Ca_2{}^{[6]}(Mg_4Al)^{[4]}[Si_6Al_2]O_{22}(OH)_2$ (Welch *et al.,* 1994, 1998) and magnesio-hornblende, $^{[A]}□^{[8]}Ca_2{}^{[6]}(Mg_4Al)^{[4]}[Si_7Al]O_{22}(OH)_2$ (Jenkins *et al.,* 1997; Hawthorne *et al.,* 2000), indicate that peaks due to MgMgAl–OH–$^{[A]}$Na (pargasite) and MgMgAl–OH–$^{[A]}$□ (magnesio-hornblende) occur at 3678 cm^{-1} and 3652 cm^{-1}, respectively. No peaks other than those observed for MgMgMg configurations were observed in the infrared spectra of the three synthetic amphiboles. As no Al is at M(1) or M(3), we infer that it is fully ordered at M(2), and this is in good agreement with the order parameter data from the simulations; the synthesis temperatures of the samples were 1023–1073 K at 1.6–2.1 GPa, and an examination of the configuration at T = 1023 K showed that only 1% of the Al atoms were not at M(2).

Discussion

We have shown by experiment that the configuration of M(1,2,3) cations in ordered glaucophane is $^{M(1)}Mg^{M(2)}Al^{M(3)}Mg$, and have used a combination of Monte Carlo simulation and *ab initio* calculations to produce the same ordered state by computation. This is a useful result, since large volumes of experimental data exist for other amphibole compositions, and such data could be used in conjunction with computational methods to investigate the crystal chemical controls on the formation of other amphibole solid solutions.

This complete ordering of $^{[6]}$Al at M(2) in glaucophane-nyböite amphiboles contrasts starkly with the high degree of disorder of Al over M(2) and M(3) sites in the calcic amphiboles pargasite and magnesio-hornblende. We note that the synthetic magnesio-hornblendes studied by Jenkins *et al.* (1997) were synthesized at 1073–1148 K (0.6–1.3 GPa), similar to the synthesis temperatures of the glaucophane-nyböite amphiboles studied here (1023–1073 K at 1.6–2.1 GPa). Therefore, one cannot simply infer that the ordered $^{[6]}$Al distribution in the latter is due to a low synthesis temperature. Rather, the highly $^{[6]}$Al-ordered state of these alkali amphiboles relative to the $^{[6]}$Al-disordered calcic amphibole magnesio-hornblende demonstrates the importance of the contribution of the M(4) cation (monovalent/divalent) in satisfying the bonding requirements at O(4). Our data show that when M(4) = Na^+ then $^{[6]}$Al is expected to be highly ordered at M(2), whereas when M(4) = Ca^{2+} a high degree of $^{[6]}$Al disorder is possible. Alkali amphiboles are, therefore, likely to be always highly $^{[6]}$Al-ordered, whereas calcic amphiboles will be highly $^{[6]}$Al-disordered at their high-temperature stability limits. We are currently extending our computational studies to aluminous calcic amphiboles using the computational methods developed here.

Acknowledgements: Monte Carlo simulations were performed at the High Performance Computing Facility of the University of Cambridge. The SIESTA calculations were performed on both the Cambridge HPCF and the computers of the UK CSAR service under a grant funded by NERC. EJP is grateful to EPSRC for financial assistance. Our Monte Carlo routines make use of a pseudo-random number generating program written by Richard Chandler (UCL) and Paul Northrop (Oxford). We thank Alison Pawley for donating her alkali amphiboles for the infrared study and Ming Zhang for assistance in the IR experiments.

References

Bosenick, A., Dove, M.T., Myers, E.R., Palin, E.J., Sainz-D´az, C.I., Guiton, B., Warren, M.C., Craig, M.S., Redfern, S.A.T. (2001): Computational methods for the study of energies of cation distributions: applications to cation-ordering phase transitions and solid solutions. *Mineral. Mag.*, **65**, 193–219.

Burns, R.G. & Law, A.D. (1970): Hydroxyl stretching frequencies in the infrared spectra of anthophyllites and gedrites. *Nature*, **226**, 73–75.

Burns, R.G. & Strens, R.G.J. (1966): Infrared study of the hydroxyl bands in clinoamphiboles. *Science*, **153**, 890–892.

Carpenter, M.A. & Salje, E.K.H (1994a): Thermodynamics of non-convergent cation ordering in minerals. 2. Spinels and the orthopyroxene solid solution. *Am. Mineral.*, **79**, 1068–1083.

–, – (1994b): Thermodynamics of non-convergent cation ordering in minerals. 3. Order-parameter coupling in potassium-feldspar. *Am. Mineral.*, **79**, 1084–1098.

Catlow, C.R.A., Cormack, A.N., Theobald, F. (1984): Structure prediction of transition-metal oxides using energy minimization techniques. *Acta Cryst.*, **B40**, 195–200.

Craig, M.S., Warren, M.C., Dove, M.T., Gale, J.D., Sanchez-Portal, D., Soler, J.M., Artacho, E. (2003): Simulations of minerals using density functional theory based on atomic orbitals for linear scaling. *Phys. Chem. Minerals* (in press).

Della Ventura, G. & Robert, J.-L. (1990): Synthesis, XRD and FTIR studies of strontium richterites. *Eur. J. Mineral.*, **2**, 171–175.

Della Ventura, G., Robert, J.-L., Raudsepp, M., Hawthorne, F.C., Welch, M.D. (1997): Site occupancies in synthetic monoclinic amphiboles: Rietveld structure refinement and infrared spectroscopy of (nickel, magnesium, cobalt)-richterite. *Am. Mineral.*, **82**, 291–301.

Gale, J.D. (1997): GULP: a computer program for the symmetry-adapted simulation of solids. *J. Chem. Soc. Faraday Trans.*, **93**, 629–637.

Hawthorne, F.C. (1983): The crystal chemistry of the amphiboles. *Can. Mineral.*, **21**, 173–480.

– (1997): Short-range order in amphiboles: a bond-valence approach. *Can. Mineral.*, **35**, 201–216.

Hawthorne, F.C., Della Ventura, G., Robert, J.-L. (1996): Short-range order of (Na,K) and Al in tremolite: An infrared study. *Am. Mineral.*, **81**, 782–784.

Hawthorne, F.C., Della Ventura, G., Robert, J.-L., Welch, M.D., Raudsepp, M., Jenkins, D.M. (1997): A Rietveld and infrared study of synthetic amphiboles along the potassium-richterite-tremolite join. *Am. Mineral.*, **82**, 708–716.

Hawthorne, F.C., Welch, M.D., Della Ventura, G., Liu, S., Robert, J-L., Jenkins, D.M. (2000) Short-range order in synthetic aluminous tremolites: An infrared and triple-quantum MAS NMR study. *Am. Mineral.*, **85**, 1716–1724.

Holland, T.J.B. (1988): Preliminary phase relations involving glaucophane and applications to high pressure petrology: new heat capacity and thermodynamic data. *Contrib. Mineral. Petrol.*, **99**, 134–142.

Jenkins, D.M., Sherriff, B.L., Cramer, J., Xu, Z. (1997): Al, Si, Mg occupancies in tetrahedrally and octahedrally coordinated sites in synthetic aluminous tremolite. *Am. Mineral.*, **82**, 280–290.

Oberti, R., Hawthorne, F.C., Ungaretti, L., Canillo, E. (1995): ^{VI}Al disorder in amphiboles from mantle peridotites. *Can. Mineral.*, **33**, 867–878.

Palin, E.J., Dove, M.T., Redfern, S.A.T., Bosenick, A., Sainz-D´az, C.I., Warren, M.C. (2001): Computational study of tetrahedral Al–Si ordering in muscovite. *Phys. Chem. Minerals*, **28**, 534–544.

Palin, E.J., Dove, M.T., Redfern, S.A.T., Sainz-D´az, C.I., Lee, W.T. (2003): Computational study of tetrahedral Al–Si and octahedral Al–Mg ordering in phengite. *Phys. Chem. Minerals,* **30**, 293–304.

Papike, J.J. & Clark, J.R. (1968): The crystal structure and cation distribution of glaucophane. *Am. Mineral.*, **53**, 1156–1173.

Pawley, A.R. (1992): Experimental study of the compositions and stabilities of synthetic nyböite and nyböite-glaucophane amphiboles. *Eur. J. Mineral.*, **4**, 171–192.

Robert, J.-L., Della Ventura, G., Thauvin, J.-L. (1989): The infrared OH-stretching region of synthetic richterites in the system Na_2O-K_2O-CaO-MgO-SiO_2-H_2O-HF. *Eur. J. Mineral.*, **1**, 203–211.

Sainz-D´az, C.I., Hernández-Laguna, A., Dove, M.T. (2001): Modeling of dioctahedral 2:1 phyllosilicates by means of transferable empirical potentials. *Phys. Chem. Minerals*, **28**, 130–141.

Sainz-D´az, C.I., Timon, V., Botella, V., Artacho, E., Hernández-Laguna, A. (2002): Quantum mechanical calculations of dioctahedral 2:1 phyllosilicates: Effect of octahedral cation distributions in pyrophyllite, illite, and smectite. *Am. Mineral.*, **87**, 958–965.

Sainz-D´az, C.I., Palin, E.J., Dove, M.T., Hernández-Laguna, A. (2003a): Ordering of Al, Fe and Mg cations in the octahedral sheet of smectites and illites by means of Monte Carlo simulations. *Am. Mineral.*, **88**, 1033–1045.

Sainz-D´az, C.I., Palin, E.J., Hernández-Laguna, A., Dove, M.T. (2003b): Octahedral cation ordering of illite and smectite. Theoretical exchange potential determination and Monte Carlo simulations. *Phys. Chem. Minerals* (in press).

Soler, J.M., Artacho, E., Gale, J.D., Garcia, A., Junquera, J., Ordejon, P., Sanchez-Portal, D. (2002): The SIESTA method for ab initio order-N materials simulation. *J. Phys. Cond. Matt.*, **14**, 2745–2779.

Warren, M.C., Dove, M.T., Myers, E.R., Bosenick, A., Palin, E.J., Sainz-D´az, C.I., Guiton, B., Redfern, S.A.T. (2001): Monte Carlo methods for the study of cation ordering in minerals. *Mineral. Mag.*, **65**, 221–248.

Welch, M.D. & Knight, K.S. (1999): A neutron powder diffraction study of cation ordering in high-temperature amphiboles. *Eur. J. Mineral.*, **11**, 321–331.

Welch, M.D., Kolodziejski W., Klinowski, J. (1994): A multinuclear NMR study of synthetic pargasite. *Am. Mineral.*, **79**, 261–268.

Welch, M.D., Liu, S., Klinowski, J. (1998): ^{29}Si MAS NMR systematics of calcic and sodic-calcic amphiboles. *Am. Mineral.*, **83**, 85–96.

Winkler, B., Dove, M.T., Leslie, M. (1991) Static lattice energy minimization and lattice-dynamics calculations on aluminosilicate minerals. *Am. Mineral.*, **76**, 313–331.

Received 29 October 2002
Modified version received 24 March 2003
Accepted 5 March 2003